Title
Multi-cyclone analysis and machine learning model implications of cyclone effects on forests

Authors
Feng, Yanlei
Negrón-Juárez, Robinson I
Chambers, Jeffrey Q

Publication Date
2021-12-01

DOI
10.1016/j.jag.2021.102528

Peer reviewed

International Journal of Applied Earth Observations and Geoinformation 103 (2021) 102528

Contents lists available at ScienceDirect

International Journal of Applied Earth Observations and Geoinformation

journal homepage: www.elsevier.com/locate/jag

Multi-cyclone analysis and machine learning model implications of cyclone effects on forests

Yanlei Feng[a,*], Robinson I. Negrón-Juárez[b], Jeffrey Q. Chambers[a,b]

[a] *University of California, Department of Geography, Berkeley, CA, USA*
[b] *Lawrence Berkeley National Laboratory, Climate and Ecosystem Sciences Division, Berkeley, CA, USA*

A B S T R A C T

Past studies of cyclones (hurricanes, typhoons, tropical cyclones) disturbance showed that meteorological, topographical, and biological factors affect the patterns of forest disturbance intensity but left open the extent to which these findings were representative across different global cyclone regions. Using remote sensing data and machine learning models, we examined how these factors change over spatial scales and assessed their consistency across four major cyclones: Katrina (August 2005), Rita (September 2005), Yasi (February 2011), and María (September 2017). Our results revealed that the factors which best explained forest disturbance intensity pattern varied across these regions. Wind speed and precipitation were the dominant factors contributing to the variation in impacts of Katrina; terrain features, especially elevation, explained most of the variation in disturbance intensity of Rita; pre-disturbance vegetation condition was significant predictors of effects of Yasi; these factors played equal roles in explaining the disturbance intensity variation of María. A 40 m/s (144 km/h) wind speed threshold was proposed to split low- and high-level forest disturbance intensity. Other than wind speed, few generalizations can be made on features across multiple regions. We built several generalized hurricane impact models, which worked well with the test data from cyclones used for model development ($R^2 = 0.89$). However, these models did not have good predictions on other cyclones, such as Michael (October 2018) and Laura (August 2020). This study showed that each cyclone interacted with the landscape in a unique way and the challenges remained in building a generalized cyclone impact model.

1. Introduction

Cyclones are one of the most disastrous weather phenomena that result in a large disturbance to forests. These extreme events produce changes in the forest structure, biomass, and species composition. The severity of forest disturbance can be quantified using the remote sensing derived disturbance metric (Chambers et al., 2007, Negrón-Juárez et al., 2010b). Studies shown that field measured tree mortality can be well represented by Landsat-derived disturbance metric ΔNPV (Negrón-Juárez et al., 2010a, 2010b, 2014a,b, Feng et al., 2020), and the spatial pattern of ΔNPV is associated with forest structures, terrain features, and meteorological factors. Factors including forest type, forest canopy height, forest age, slope, elevation, aspect or wind exposure, wind speed, storm precipitation, antecedent rainfall have shown significance in explaining the spatial variation in forest disturbance intensity metric (Hall et al., 2020, Feng et al., 2020, Negrón-Juárez et al., 2010b, 2014a, b, Kim et al., 2019).

Recent studies show that wind and rainfall are strong predictors for forest disturbance intensity (Hall et al., 2020, Negrón-Juárez et al., 2014a,b). Climate change enhances hurricane-related rainfall and increases the activities of north Atlantic hurricanes. Future anthropogenic warming will increase the number of intense tropical cyclones, wind speed and extreme rainfall rate associated with storms (Goldenberg et al 2001, Kossin 2018, Patricola and Wehner 2018). Wetter and more severe storms exert strong pressure on forests (Hall et al., 2020; Uriarte et al., 2019). Therefore, it is important to understand how wind and rainfall affect forest disturbance directly and how these effects are altered by other factors, including terrain features and forest structures. More important, as the trend of poleward migration of the locations of tropical cyclones maximum intensities become more and more evident (Kossin et al., 2014), the exploration of how the factors affecting spatial pattern of forest disturbance intensity vary by different regions where cyclones made landfall is necessary.

It is challenging to reveal the physical process of wind and forest disturbance through low resolution climate data (~kilometers) and high resolution forest changes images (30 m). Moreover, the process is affected by variables at different scales, including terrain features, forest structure, and soil properties, making it difficult to explore how the features affect the pattern of disturbance intensity. Most forest disturbance studies associated with tropical cyclones focus on explaining disturbance variance at the fine scale (per tree) using field surveys and ground-based measurement. Xi et al., (2008a) found that our ability to

* Corresponding author.
E-mail address: ylfeng@berkeley.edu (Y. Feng).

https://doi.org/10.1016/j.jag.2021.102528
Received 10 April 2021; Received in revised form 18 August 2021; Accepted 26 August 2021
Available online 1 September 2021

predict tree damage increases with spatial scale. Remote sensing provides a chance to examine the geographical patterns of risk factors for broad-scale disturbances. There are a number of studies address the potential for using remote sensing to develop disturbance intensity maps at larger scales (Dolan et al., 2011, Negrón-Juárez et al., 2014a,b; Feng et al., 2020; Gang et al., 2020; Hall et al., 2020). However, no study explains how these features affect the forest disturbance differently across multiple regions.

Most studies in wind and forest disturbance employed parametric models, which assumed data follow a normal distribution (e.g. multiple linear regression in Feng et al., 2020). Traditional statistical models such as linear regression and logistic regression deliver excellent results when dealing with unimodal data; However, data gathered from satellites rarely follow normal distribution, especially in a multi-variate model (Belgiu and Drăguţ, 2016, Breiman 2001). Simple parametric models imposed on data generated from complex system would result in loss of accuracy and information (Breiman 2001). Therefore, non-parametric models, such as the Classification and Regression Tree (CART), Support Vector Machine (SVM), and Neural Network (NN), which do not make assumptions regarding data distribution, gained popularity in remote sensing data analysis (Belgiu and Drăguţ, 2016). Recent advances in machine learning offer new opportunities in earth system science field, which benefit from rich geospatial data provided by satellite images and climate model simulation. Machine learning methods extract patterns and insights from the data, and the approaches have been proved successful in land use and land cover classification (Gislason et al., 2006), anomaly detection (Russo et al., 2020), and regression estimation of biogeophysical parameters at local and global scales (Hall et al., 2019). Therefore, it is exciting to use machine learning to reveal the links between remote sensing images derived forest disturbance intensity and the factors, including wind and rainfall, forest structure, terrain features, and soil properties.

The objectives of this study were to compare four regions in continental US, Caribbean island, and coastal Australia that experienced severe cyclones and explore how the features alter the disturbance intensity pattern in multiple ways at different regions. In this paper, we also discussed the possibility to build a machine learning model to predict the impact of an unseen hurricane on forests based on meteorological variables, and existing data of forest and terrain features. Our machine learning model used 13 predictors (Table 1, additional details in Table S2, Fig. S1.1–S1.13) from landscape, vegetation, climate, and soil variables, including Green Vegetation ratio in preceding year (PreGV), elevation, aspect, slope, canopy height, precipitation, forest type, wind, topographic diversity, landform, wetness, soil water, soil texture. The predictors were chosen based on literatures and limited by the spatial and temporal coverage of the data. The model used Landsat-derived forest disturbance intensity metric as the independent variable. We used data of four major cyclones to build the model: Hurricane Katrina (2005) and Rita (2005) in Mexico Gulf coast, tropical cyclone Yasi (2011) in Australia, and hurricane María (2017) in Caribbean Sea.

Table 1
Predictors of cyclone impact on forests.

Predictors	Data Type	Data Source
Wind	Climate variables	H*wind, HURRECON
Precipitation		Daymet
Elevation	Terrain features	SRTM DEM
Aspect		
Slope		
Landform		
Topo-diversity		
Canopy height	Forest properties	GLAS
Land cover		MERIS
PreGV		The author
Soil water	Soil properties	Hengl and Gupta, 2019
Soil texture		Hengl and Gupta, 2019
Wetness		MODIS

Hurricane Michael (2018) and Laura (2020) were used as test data. In the following chapters, we first explored the relationship between landscape features, climate, soil, forest type and forest disturbance intensity metric over different regions. Then we built individual machine learning model to extract the feature importance of each cyclone. Next, we built a general cyclone model and tested on an unseen hurricane Michael. In the end we tested the models on unseen hurricane Laura which occurred in the same region as Rita. (Hereafter all tropical cyclones will be referred by their names.)

2. Study areas and hurricane cases

We investigated the impact of hurricanes on forests grown on Continental US, Australia, Puerto Rico island in the Caribbean Sea (Fig. 1).

2.1. Continental US - Hurricane Katrina, Rita, Laura, Michael

Katrina made landfall on southeast Louisiana and passed through coastal Mississippi on August 29, 2005 with maximum sustained wind speeds of 180–200 km/h. Shortly after, Rita made landfall near the border of Texas and Louisiana on September 24, 2005, with maximum sustained winds of 193 km/h. With little variation in terrain and low elevation coastal zones (Board, 2018), hundreds of kilometers of the coast were affected by storm surges of more than 3 m brought by these two cyclones. 15 years later, Laura followed a similar path as Rita, with stronger intensity and higher sustained wind near 240 km/h, brought over 5 m storm surge.

Michael made landfall on October 10, 2018, near Mexico Beach in Florida, with maximum sustained winds of 257 km/h. It is the first Category 5 storm on modern record in the Florida Panhandle region.

2.2. Australia rainforest – Tropical cyclone Yasi

Yasi made landfall on Feb 3rd, 2011 on the northern tropical coast near Mission Beach, Queensland. It maintained a strong core with damaging winds estimated up to 285 km/h. The peak storm surge was estimated at ~ 7 m and inundated over 300 m inland (Perry et al., 2014). Great variance of elevation exists in this region, and the highest elevation is over 1000 m.

2.3. Caribbean island – Hurricane María

María made landfall near Yabucoa Harbor, southeast Puerto Rico on September 20, 2017. Its maximum sustained wind speed reached 250 km/h. Puerto Rico is a mountainous island, and annual precipitation

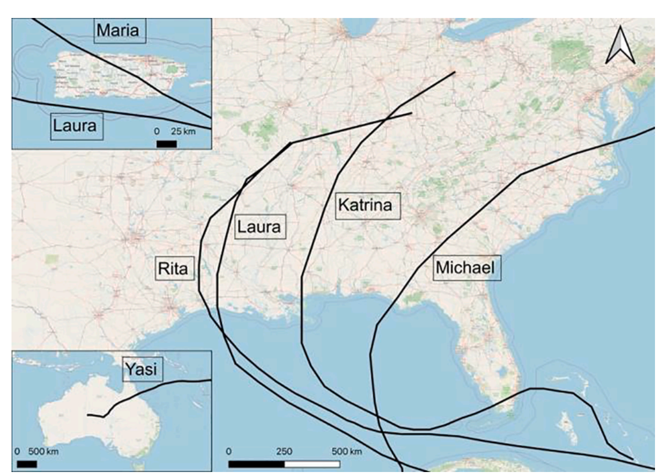

Fig. 1. Tracks of Katrina, Rita, Yasi, and Maria used for model development, Michael and Laura used for model test.

varies from southwest (750 mm) to northeast (1500–2000 mm). Highest annual precipitation with over 4000 mm was found in the higher elevations of Luquillo Experimental Forest (Birdsey and Weaver 1982, Boose et al., 2004). Storm surge and tide produced inundation along the coastal Puerto Rico, with the maximum inundation at south-eastern coasts (NHC, 2018).

3. Data

3.1. Forest disturbance intensity metric

We employed the method from Chambers et al. (2007) to generate forest disturbance intensity maps using satellite images. We collected Landsat surface reflectance images from Google Earth Engine platform for both pre-hurricane and post-hurricane images of each hurricane (Table 2). The time ranges were selected for pre and post hurricane images to minimize the effect of seasonal phenology and generate cloud-free images. Topographic Illumination was applied on Landsat images to minimize the illumination effects (shadow, slope, etc.) due to topography (Tan et al., 2013). Then Landsat images were radiometric calibrated band by band with respect to invariant targets from urban area. After pre-processing, the image collections were composited to two pre- and post-hurricane images by selecting the mean. Then spectral mixture analysis (SMA) (Adams et al., 1995) was conducted on the pre and post images using Landsat-derived endmembers (see detailed process in Feng et al., 2020), including green vegetation (GV), non-photosynthetic vegetation (NPV), and shade. Pre- and post-hurricane images of the same region where hurricane passed shared its own endmember spectra. After shade normalization, changes in NPV (ΔNPV) were calculated to represent the forest disturbance intensity (Fig. 2). Past studies showed that there was a strong correlation between field measured tree mortality and Landsat-derived forest disturbance intensity (ΔNPV) from forests affected by Katrina (Chambers et al., 2007), Rita (Negrón-Juárez et al., 2014a,b), Yasi (Negrón-Juárez et al., 2014a; Negrón-Juarez et al., 2014b), and María (Hall et al., 2019; Feng et al., 2020). Therefore, our research focused mainly on these four cyclones and they were used as the training data for the model development. Michael and Laura were only used as unseen cyclones for testing the model.

3.2. Climate variables

We used Daymet Daily Surface Weather Data precipitation data, which were model-produced gridded surfaces of daily weather parameters based on observations from meteorological station (Thornton et al., 2016). Daily total precipitation band from Daymet was selected. Wind surface data were collected using H*wind model (Powell et al., 1998). H*wind model uses wind measurements from multiple observation stations. H*wind data are available for Katrina, Rita, Yasi, and María. For two case studies Michael and Laura, HURRECON model (Boose et al., 2001) was employed to estimate wind speed and wind duration, as a function of cyclone track and maximum sustained wind speed.

Table 2
Cyclones' Satellite Image Collection.

Cyclone Name	Satellite	Pre-cyclone Collection	Post-cyclone Collection
Katrina	Landsat 5	Sep 1st to Dec 31st, 2004	Sep 1st to Dec 31st, 2005
Rita	Landsat 5	Oct 1st to Dec 31st, 2004	Oct 1st to Dec 31st, 2005
Yasi	Landsat 5	Feb 1st to June 30th, 2010	Feb 1st to June 30th, 2011
María	Landsat 8	June 1st to Sep 30th, 2016	Oct 1st ,2017 to Jan 30th, 2018
Michael	Landsat 8	Sep 1st to Dec 31st, 2017	Oct 1st ,2018 to Jan 30th, 2019
Laura	Landsat 8	Sep 1st to Dec 31st, 2019	Sep 1st to Dec 31st, 2020

3.3. Terrain features

Elevation, aspect, and slope data were retrieved from the Shuttle Radar Topography Mission (SRTM) digital elevation (DEM) dataset (Jarvis et al., 2008). SRTM also provides the landform classes, including peak, mountain, cliff, slope, etc. (Theobald et al., 2015). Topographic diversity data are also based on SRTM DEM, and the data represents the temperature and moisture condition of local habitat to species. Higher topographic diversity should support higher diversity of plants (Theobald et al., 2015).

3.4. Forest properties

Global forest canopy height data are based on a fusion of spaceborne-Lidar data from the Geoscience Laser Altimeter System (GLAS) and ancillary geospatial data (Simard et al., 2011). The landcover map that has 22 land cover classes is derived by regionally tuned classification based on ENVISAT's Medium Resolution Imaging Spectrometer (MERIS) (ESA and UCLouvain, 2010). PreGV variable, which represents the green vegetation ratio in the preceding year of cyclone, were generated using SMA.

3.5. Soil properties

Soil water variable shows the soil water content (volumetric %) for 33 kPa suctions predicted at 0 cm depths (Hengl and Gupta, 2019). Soil texture variable represents the soil texture classes at 0 cm depth, including Cl, SiCl, SaCl, ClLo, etc (Hengl, 2018). The wetness data are gap-filled tasseled cap wetness based on MODIS BRDF-corrected imagery (MCD43B4).

4. Methods

4.1. Pre-processing data

Multi-band image data were reshaped into 2d tabular data using 30 m as the resolution of each pixel. Since we only focused on positive ΔNPV that indicating immediate forest damage, we cleaned NaN values and extreme values, including pixels with ΔNPV over 1 or below 0 and pixels with preGV over 1 or below 0. Excluded negative ΔNPV represented forests greening after cyclones, and other pixels with extreme values (>1 and < -1) may result from sensor errors or atmospheric illumination effects. Then the data were normalized using standard normalization and one hot encoder function was applied to deal with the categorical data.

4.2. Sampling methods

Sample size, quality, and sample selection methods can affect regression result and prediction accuracy (Ramezan et al., 2019). The data distribution of cyclone disturbance intensity in multiple regions show a similar pattern with a huge amount of low intensity disturbance and a small portion of high intensity (Fig. 3). To choose the training data that can be representative of different levels in the extreme right-skewed histogram of disturbance intensity, appropriate sampling methods and a large sample size are required.

Here we tested four sampling methods with the sample size of 50,000 pixels:

1) Simple random sampling: a purely random selection of 50,000 samples is selected from the data with replacement. While the samples give a direct estimate of the population parameters, this method exacerbates the difficulty dealing with long tail of data.

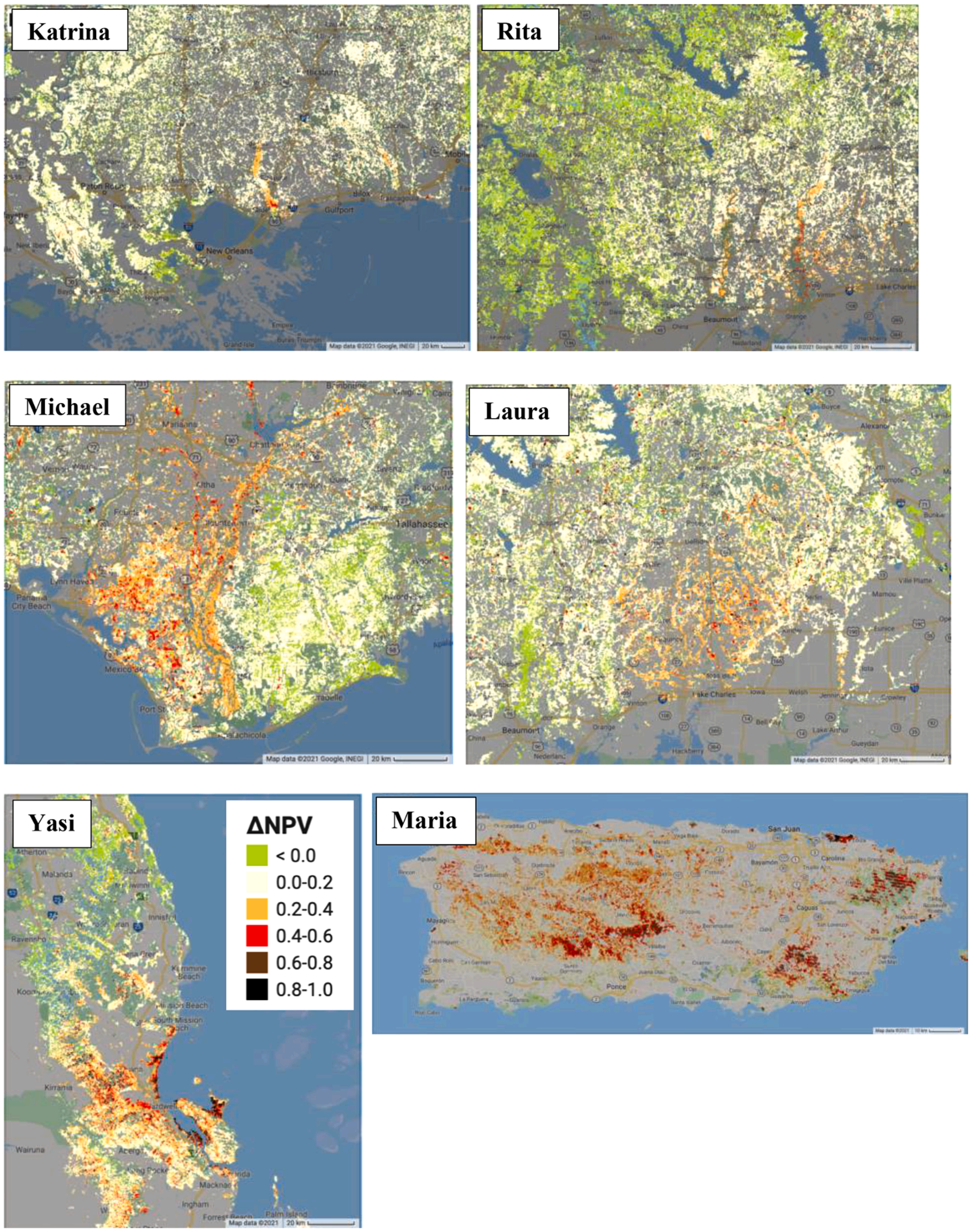

Fig. 2. Disturbance intensity map of hurricane disturbance. Katrina, Rita, Yasi, María have been validated with field observations and high-resolution airborne remote sensing images. UI Interface: https://ylfeng.users.earthengine.app/view/jagfengetal.

2) Equalized stratified sampling: The response values ΔNPV, range from 0 to 1, are divided into 5 stratum (0.2 in each strata), and 10,000 samples are drew from each of the strata with replacement. Since sometimes the desired sample sizes are larger than the population of the minority stratum, sampling with replacement will generate duplicate examples in the minority groups, which may result in model overfitting. A followed cross-validation method prevents the model from overfitting.
3) Disproportional stratified sampling: The size of the strata is specified by user. 32000, 16000, 8000, 4000, 2000 samples are selected in the strata from lowest level disturbance population to highest level disturbance (0.2 in each strata).
4) Simple random sampling on high level disturbance intensity: a purely random selection of 50,000 samples is selected from the data with ΔNPV value larger than 0.3. This method focuses only on high level disturbance intensity.

4.3. Random forest

We employed random forest (RF) (Breiman 2001) in this research. RF uses a set of decision trees to make prediction. Different from decision trees, RF grows many trees using a bootstrap approach to draw a subset of training samples from the original training dataset. This bootstrap approach aggregating over a forest of trees can reduce instability while improving accuracy. Moreover, RF draws a random selection of a user-defined number of input variables at each split to find the best split. At the end of the leaf node, the average of the observations within the area is computed. RF provides the feature importance by computing how much each feature contributing to the average decrease in impurity or

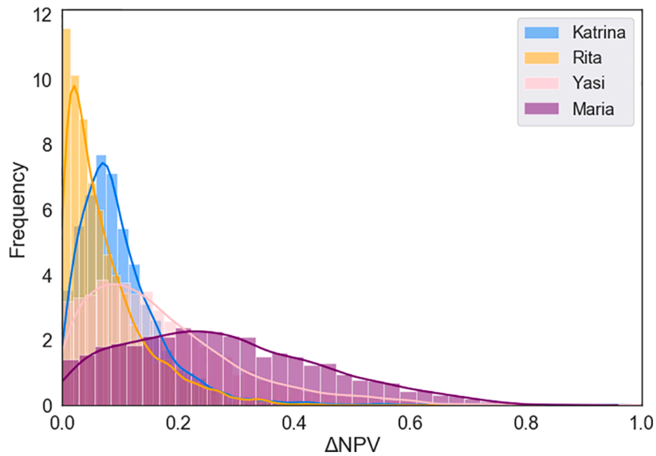

Fig. 3. Histogram and probability density function of ΔNPV show a right-skewed distribution pattern.

variance over trees.

Random forest is chosen with the best performance with lowest error and highest R2 on the training data among candidate models, including linear regression, lasso, ridge, decision tree, support vector machine, 3 layers deep neural network (Table S1).

4.4. Cross validation

Cross validation is a model validation technique that splits the data several times and estimates the error by averaging over the hold-out sets to avoid overfitting. A cross validation were performed on each cyclone dataset.

4.5. Prediction performance metric

Two metrics were calculated to quantify prediction performance: r^2 and normalized root mean square error (RMSE). The r^2 of each regression model indicates the percentage of variance in response value the model explained. The normalized RMSE between predicted ΔNPV and satellite-derived ΔNPV was reported. It is a standard and robust measure of error.

5. Results and discussion

5.1. Data exploration

5.1.1Wind

The effect of wind speed on forest disturbance intensity was investigated. Fig. 4 displays the relationship between wind speed and disturbance intensity of Katrina, Rita, Yasi, and María. Wind speed was strongly correlated with ΔNPV (mean $r = 0.26$, $p < 0.01$) across all cyclones. The plots show that ΔNPV slightly increased with wind speed smaller than 40 m/s. There is a significant increase in disturbance intensity with wind speed approaching 40 m/s or even stronger. With weaker wind speed smaller than 40 m/s, both Katrina and Yasi have relatively low level disturbance. High disturbance intensity is found on the pixels that experienced strong wind speed greater than 40 m/s. 90% of Katrina pixels that have over 50% forests impacted experience strong wind at a minimum of 39.72 m/s, while same impact has found in Yasi pixels with stronger wind at a minimum of 41.41 m/s. The maximum wind speed of Rita is 33.98 m/s, which is associated with relatively low level disturbance. 99% Rita sampling pixels have ΔNPV smaller than 0.32. Different from Rita, María has high level disturbance in general, since 75% of sampling pixels experience wind speed over 45 m/s.

5.1.1. Precipitation

Fig. 5 shows the relationship between precipitation and ΔNPV. The amount of precipitation varies a lot across these four major cyclones. Katrina has a big range of precipitation over the region with mean daily precipitation of 75.23 mm. Rita has intensive daily precipitation with mean of 174.81 mm. 75% of Rita sampling pixels experience nearly 160 mm daily rainfall. Different from Rita, Yasi has low precipitation with mean daily precipitation of 30.39 mm and max 50 mm. María also has a big range of precipitation between 32 mm and 200 mm. Over half of María sampling pixels receive 200 mm precipitation on the day of cyclone landfall.

High level impact on forests is associated with extreme precipitation. 90% of Katrina forested sampling pixels which have ΔNPV greater than 0.5 experience over 157 mm daily rainfall. Top 10% highest impacted forest pixels over the region of Rita has a minimum of 150 mm rainfall. There is an increasing trend of ΔNPV associated with increase of rainfall of Katrina. Similar positive correlation was also found on Yasi and María.

5.1.2. Elevation

Elevation is another factor that play an important role in explaining the variance in disturbance intensity ($p < 0.01$), but it varies greatly across different impacted regions, probably due to the effects of topography on wind speed and direction. US gulf coast affected by Katrina and Rita are flat with highest elevation <200 m. A negative correlation between elevation and ΔNPV suggests forests on lower regions in Gulf coasts maybe prone to damage. Northeastern Australia rainforests and Puerto Rico, affected by Yasi and María, have great range of elevation, ranging from 0 to 1400 m. Clear patterns were observed that forest disturbance intensity is positively correlated with elevation in Puerto Rico, and highest disturbance were found in mountainous areas with high elevation (Feng, Negrón-Juárez, and Chambers, 2020). As observed in Fig. 6, disturbance severity decreases as the elevation increases from 600 to 1500 m over the region affected by Yasi (also mentioned in Negrón-Juárez et al., 2014a,b). However, no clear pattern between elevation and disturbance can be observed on other cyclones.

5.1.3. Green vegetation ratio in the preceding year

Similar patterns can be found between preGV and ΔNPV across four cyclones (Fig. 7). Most disturbance effects were detected on the forest pixels with high ratio of green vegetation in the preceding year (preGV). 75% of samples that impacted by Katrina have over 77% of vegetation cover in the year before cyclone hit. Similar impacts were found on Rita (76% preGV) and María (79% preGV). A strong positive correlation can be observed between preGV and ΔNPV on Katrina ($r = 0.34$, $p < 0.01$), Yasi ($r = 0.09$, $p < 0.01$), and María ($r = 0.18$, $p < 0.01$, also mentioned in Feng, Negrón-Juárez, and Chambers, 2020). High disturbance intensity was found in the area with high green vegetation ratio in the preceding year, which indicates that areas with high percentage of forests are more likely to experience severe cyclone impacts. PreGV is also strongly correlated with ΔNPV on Rita ($p < 0.01$), but no clear positive correlation was observed.

5.2. Feature importance and sampling sensitivity

We used random forest to train four models independently on data of Katrina, Rita, Yasi, and María, and then we generated the impurity-based feature importance. In addition, we tested four different sampling methods for each cyclone. Therefore, we have 16 models in total. We trained models with 800–1000 estimators and 2 min sample splits. We employed 4-fold cross validation to estimate the skills of the model. In addition, bias and variance plots were checked to make sure there was no overfitting in the models. The results are displayed in Table 3.

During 4-fold cross-validation, the models displayed strong ability to estimate ΔNPV (average $R^2 \sim 0.8$, average RMSE $\sim 10\%$). The models show high importance in climate, terrain, and forest variables, and low

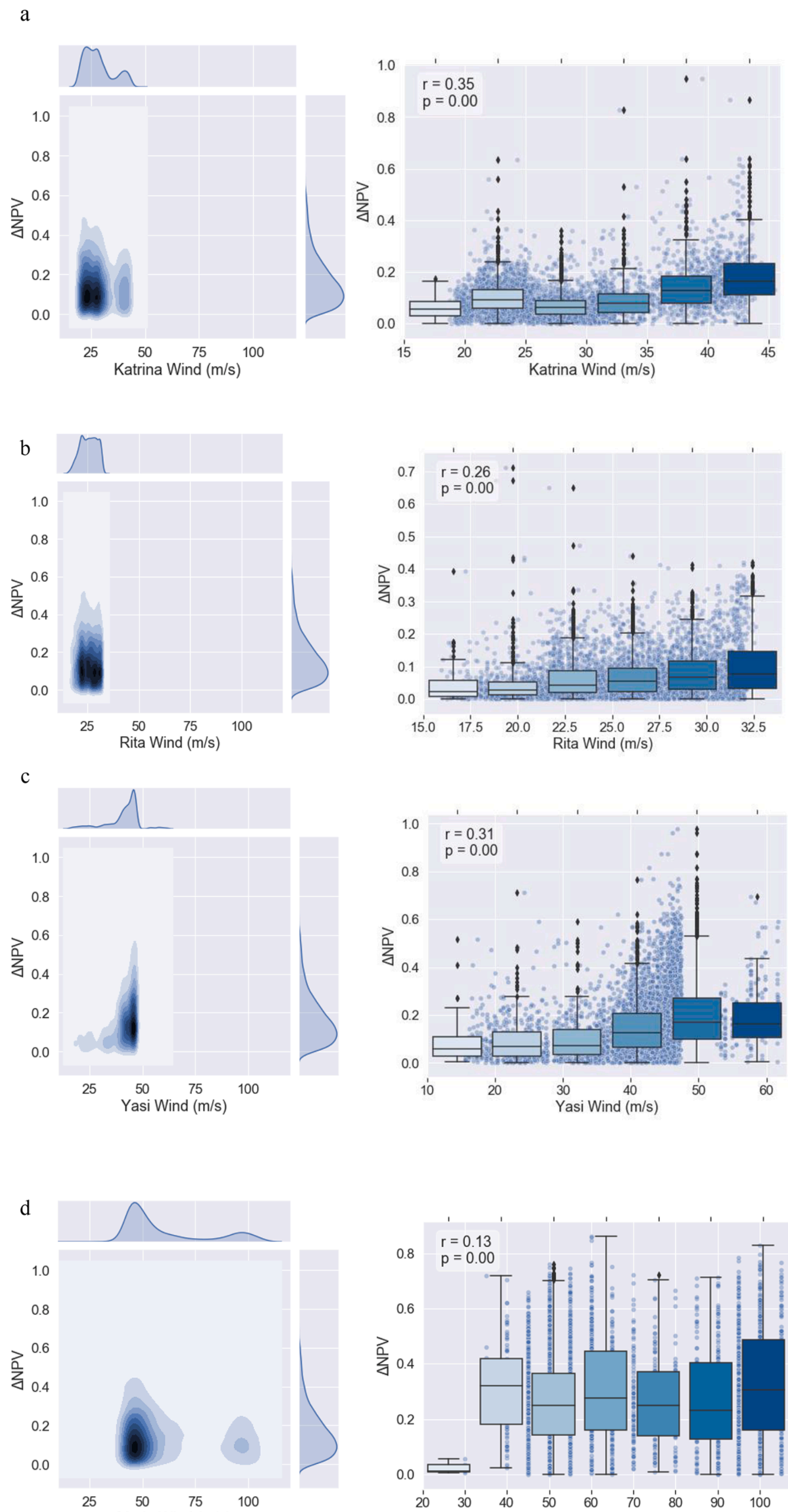

Fig. 4. The variation in the disturbance intensity ΔNPV with respect to wind speed (m/s) of (a) Katrina, (b) Rita, (c) Yasi, (d) María. Same × axis scale was applied for kernel density plots on the left. Different scales were suited to data of each cyclone on the histogram plots on the right.

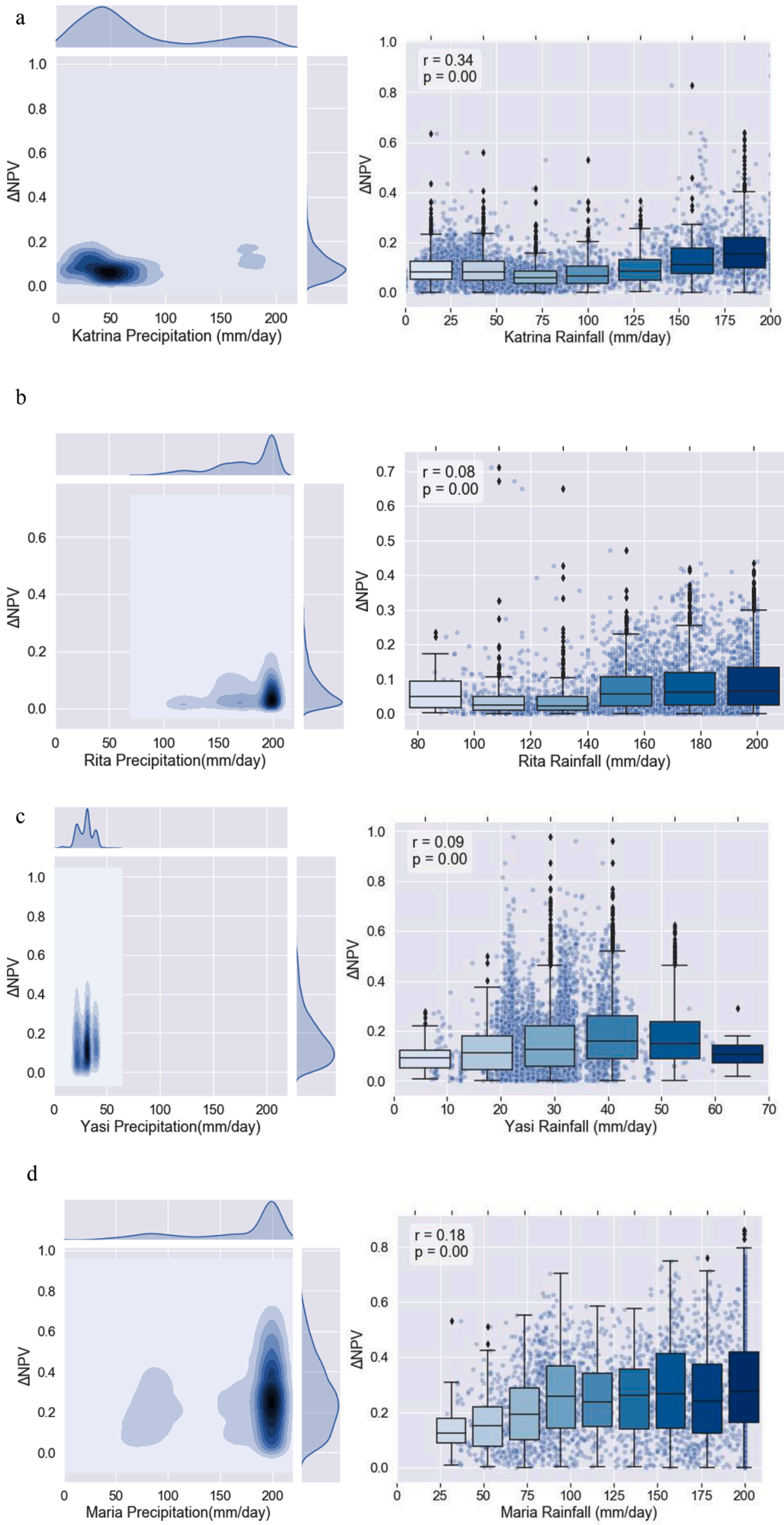

Fig. 5. The variation in disturbance intensity (ΔNPV) with respect to rainfall among (a) Katrina, (b) Rita, (c) Yasi, and (d) María.

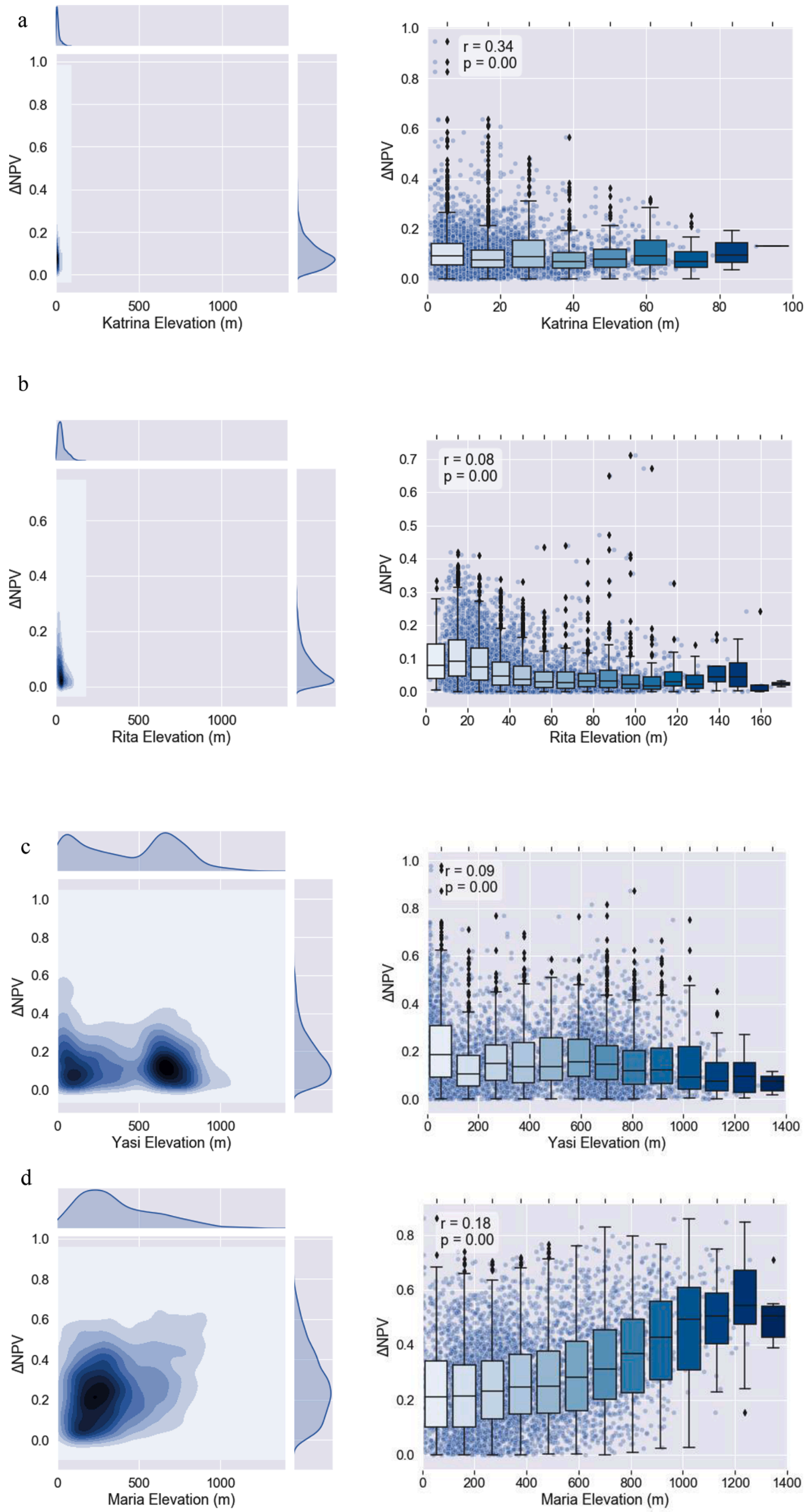

Fig. 6. The variation in disturbance intensity (ΔNPV) with respect to elevation among (a) Katrina, (b) Rita, (c) Yasi, and (d) María.

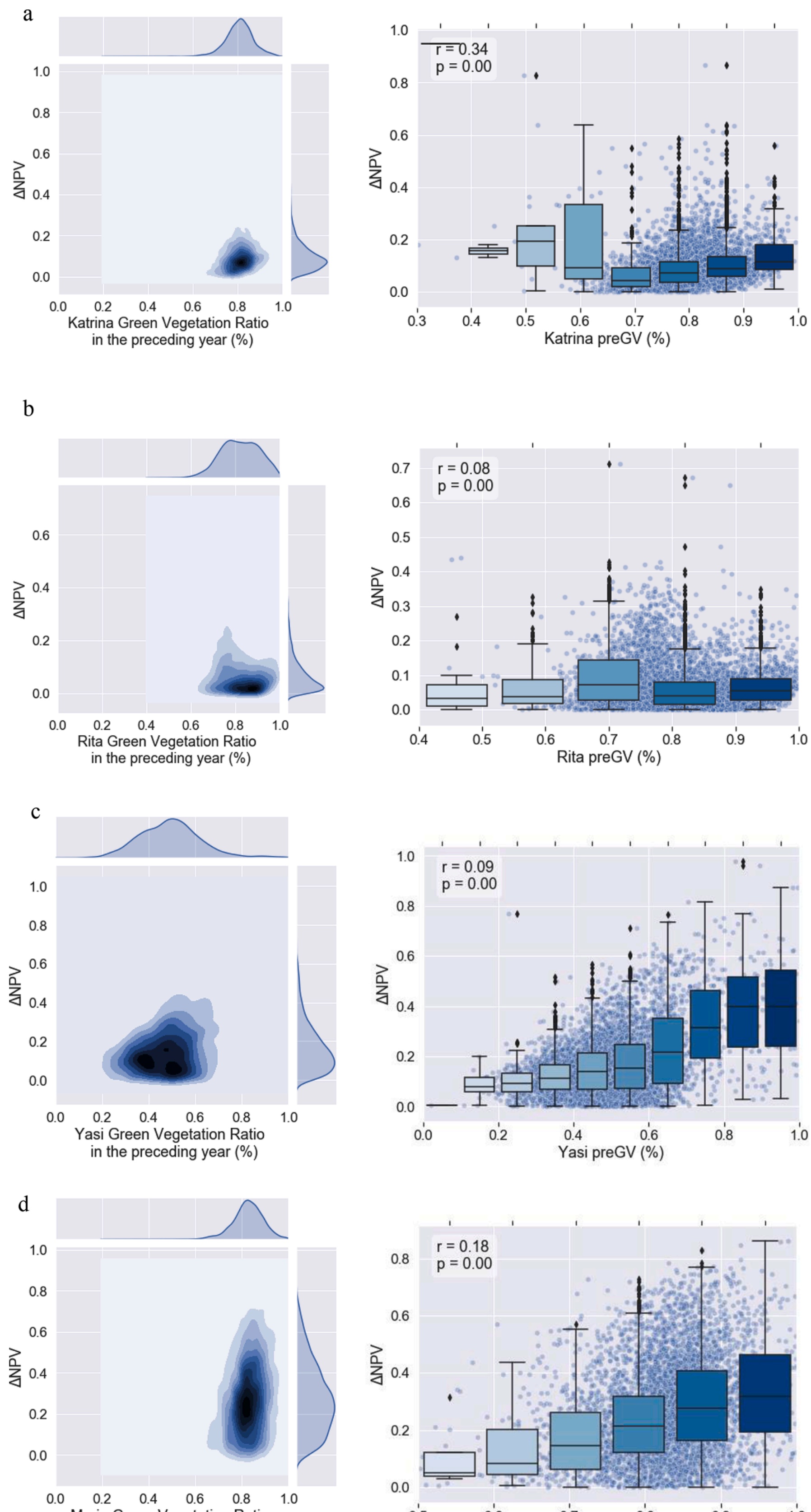

Fig. 7. The variation in disturbance intensity (ΔNPV) with respect to green vegetation ratio in the year before (a) Katrina, (b) Rita, (c) Yasi, and (d) María.

Table 3
Model performances using multiple sampling methods on four cyclones.

	Cyclone Models	Simple Random Sampling	Disproportional stratified sampling	Equalized stratified sampling*	Simple Random y > 0.3*
RMSE	Katrina	5.00%	9.62%	/	/
	Rita	5.60%	8.10%	/	/
	Yasi	8.86%	10.7%	12.7%	7.97%
	María	13%	13%	12.9%	8.15%
R^2	Katrina	0.60	0.81	/	/
	Rita	0.43	0.87	/	/
	Yasi	0.58	0.75	0.79	0.54
	María	0.41	0.76	0.61	0.46

*Katrina and Rita models were not trained using equalized stratified sampling and random sampling with y > 0.3 methods due to few samples had ΔNPV over 0.3.

importance in soil variables. The following sections show the variety of feature importance in each model.

5.2.1. Katrina model

The model with disproportional stratified sampling method (DSS) has the best performance on predictions with high R^2 (0.81) and relatively low RMSE (9.62%). Fig. 8b shows the correlation between predicted ΔNPV and observed ΔNPV. Wind and canopy height are the most important two factor affects the forest disturbance variance caused by Katrina (Fig. 8a). Over 30 percent of model variance is explained by wind. Canopy height plays a more important role in the model with disproportional stratified samples than the model with random sampling. The former model has much more samples in high level disturbance than the latter, which suggests that canopy height explains the variation in ΔNPV better in high level disturbance. Past studies also showed that there was a significant negative correlation between post-Katrina mean canopy height and ΔNPV (Dolan et al., 2011).

5.2.2. Rita model

Rita model with disproportional stratified sampling predicts ΔNPV with high accuracy (RMSE = 8.10% and R2 = 0.87), which achieves better performance than the model with simple random sampling (RMSE = 5.60% and R2 = 0.43). For Rita model, elevation is the most significant factor, followed by wind, preGV, and precipitation (Fig. 9a).

5.2.3. Yasi model

The two models with stratified sampling methods have the best performance (Equalized stratified sampling: RMSE = 12.7% and R2 = 0.80; Disproportional stratified sampling: RMSE = 10.7% and R2 = 0.75) in predicting disturbance intensity that caused by Yasi. PreGV accounts for more than 40% of variance in Yasi model, followed by wind, elevation and topographic diversity (Fig. 10a). This was consistent with previous Yasi impact on forests analysis that the terrain features, including elevation, aspect, slopes, have large impact on the pattern of forest disturbance, and complex terrain interactions speed up wind at higher elevation (Negrón-Juárez et al., 2014b).

5.2.4. María model

With the highest disturbance samples in the four training dataset, María model with equalized stratified sampling has the best performance with high R2 (~0.76) and low RMSE (~13%). María model shows relative balanced feature importance in most features. The most important features are elevation and preGV, closely followed by wetness (Fig. 11a). Each of precipitation, wind, topographic diversity, and wetness accounts for approximately 10% variety in María model.

Overall, the models are able to predict wind disturbance in multiple regions with small mean square error. There is a high correlation between predicted values and true values in these models. The predicted values tend to be smaller than true values at high disturbance level in all the models, indicating these models may underestimate the forest disturbance intensity caused by cyclones.

5.3. A general cyclone disturbance impact model

We combined data from Katrina, Rita, Yasi, and María to train a general model. Equalized stratified sampling was selected to handle the imbalanced training data caused by fewer observation points in high disturbance categories in Katrina and Rita. We used ~ 300,000 observation samples in a random forest model with 100 estimators and 4-fold cross validation.

Overall, the random forest model is able to predict test data from these four cyclones with a mean error close to zero and standard deviation of ~ 0.09 (Fig. 12 b). The average RMSE reported by the model is 9.12%, outperforming most of individual cyclone models in section 5.2. There is a high correlation (R^2 = 0.89) between predicted disturbance intensity and observed intensity. The regression performance is also worse at high level disturbance intensity than low level (Fig. 12 a).

5.4. Test the general cyclone model on Michael

To evaluate the performance of this general cyclone model on a

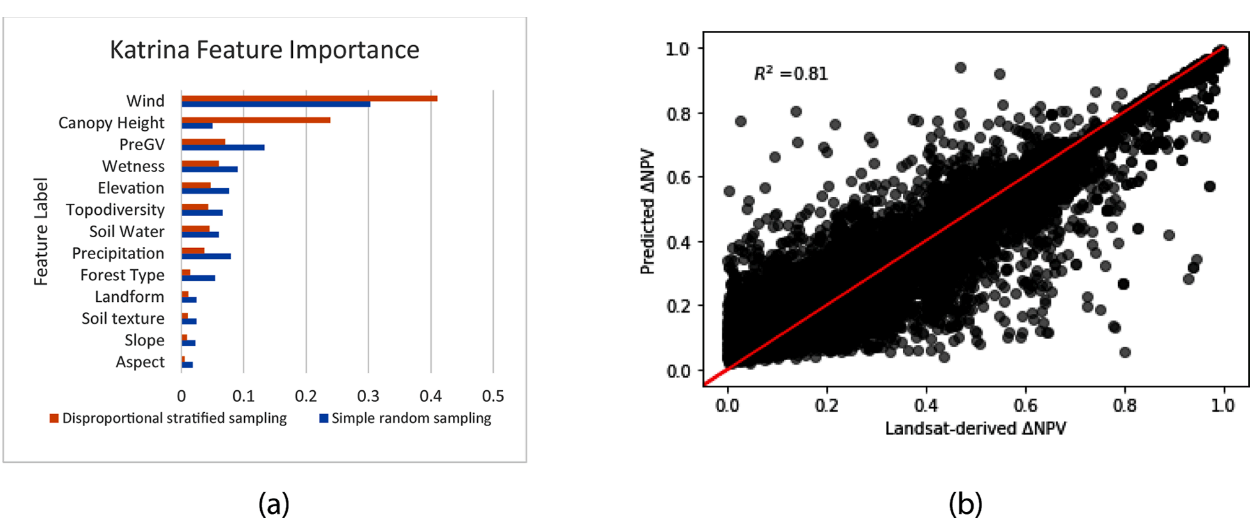

Fig. 8. (a) Feature importance of Katrina model using simple random sampling and disproportional stratified sampling methods. (b) The correlation between predicted ΔNPV from disproportional stratified sampling model and Landsat derived ΔNPV.

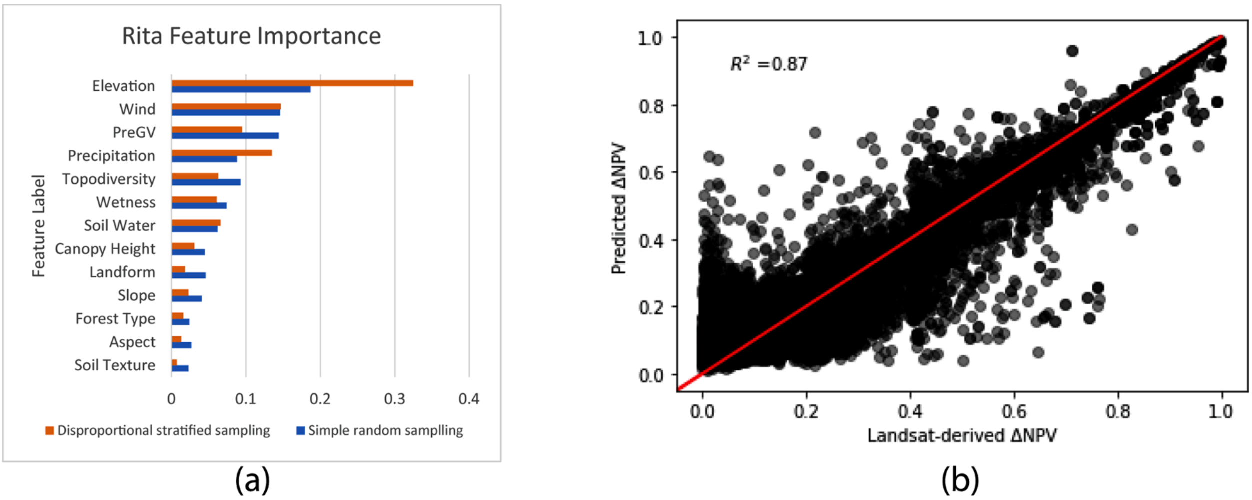

Fig. 9. (a) Feature importance of Rita model using simple random sampling and disproportional stratified sampling methods. (b) The correlation between predicted ΔNPV from disproportional stratified sampling model and Landsat derived ΔNPV.

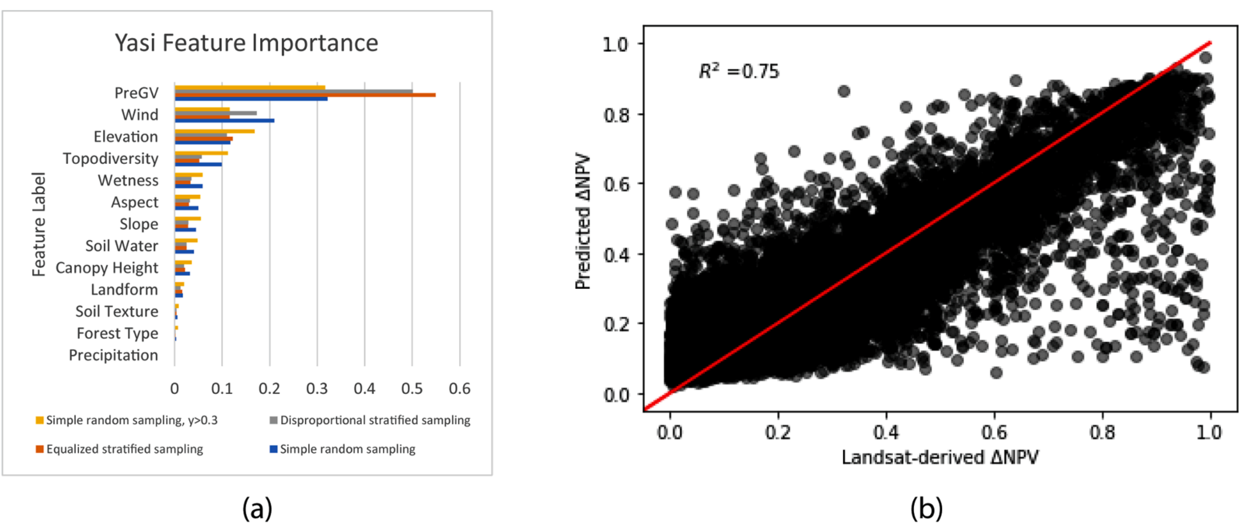

Fig. 10. (a) Feature importance of Yasi model using multiple sampling methods. (b) The correlation between predicted ΔNPV from disproportional stratified sampling model and Landsat derived ΔNPV.

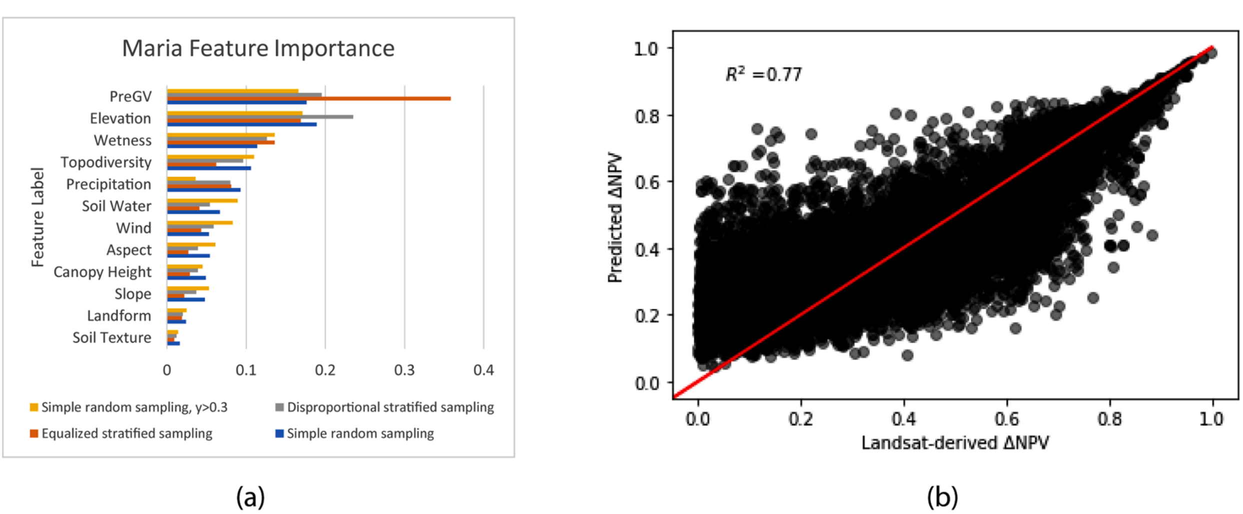

Fig. 11. (a) Feature importance of Maria model using multiple sampling methods. (b) The correlation between predicted ΔNPV from equalized stratified sampling model and Landsat derived ΔNPV.

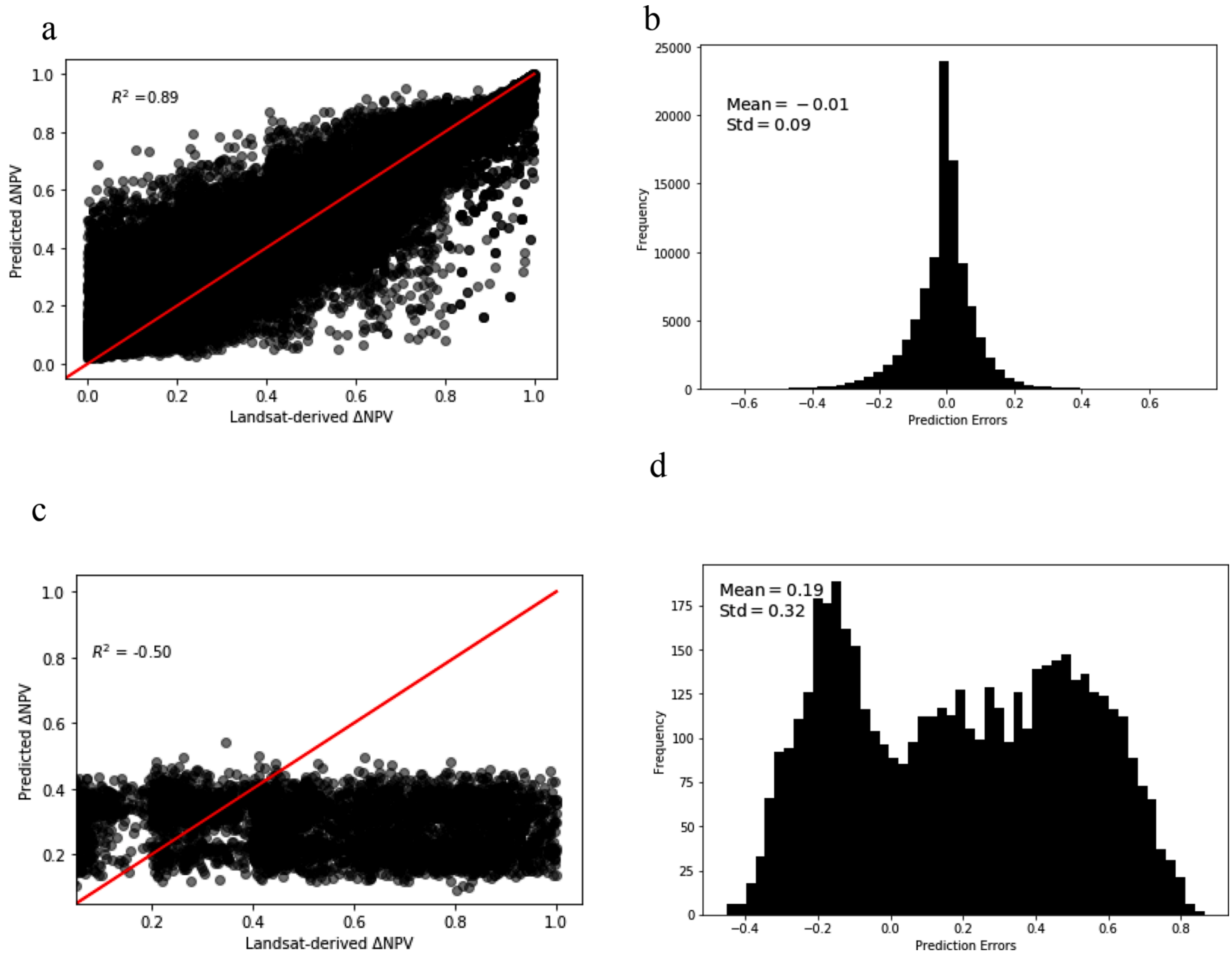

Fig. 12. The correlation between predicted ΔNPV and observed ΔNPV on (a) hold out test data (r^2 = 0.89), (c) test data from Michael (r^2 = -0.5); Prediction error plots on (b) hold out test data, (d) test data from Michael.

completely unseen cyclone, we selected cyclone Michael as our test cyclone. Cyclone Michael predictions based on the general cyclone impact model are shown in Fig. 12c and d. The RMSE of the prediction is 36.80%, indicating that the model has poor performance on predicting cyclone Michael disturbance intensity. Comparing the predicted ΔNPV with Landsat derived ΔNPV, the negative R^2 suggests that the model is even worse than a constant model. Fig. 12d shows that mean error is close to 0.19 and a standard deviation of 0.32.

The performances of the general cyclone impact model indicates that the cyclone model works well when train and test data are in the same area and works not well on an unseen cyclone.

5.5. Test the models on Laura

In 2020, Cyclone Laura took a similar path as Rita in 2005. Both cyclones affected southwest Louisiana, and Laura was the first Category 4 cyclone ever hit the region. We trained three models on existing cyclone impact data and tested if they can be further applied to an unseen cyclone that occurred in a similar region. The three models were trained using 1) Rita data; 2) both Rita and Katrina data (both cyclones were in US gulf coasts); 3) all existing cyclones data. Disproportional stratified sampling was applied to these models.

All the three models had minimum effect on predicting Laura, with a highest R^2 of 0.006 and lowest RMSE of 23.5% (Table 4). The failure of these three models indicates that even if the test cyclone is in the same region as training cyclone data, the models still lack the ability to predict the impact of an unseen cyclone.

Table 4
Model performances on Laura.

Training data	Rita	Katrina & Rita	All
RMSE	0.259	0.235	0.244
R^2	−0.312	0.006	−0.062

6. Discussion

6.1. Feature Importance, sampling methods, and forest disturbance

Cyclone disturbance intensity data has a highly right skewed distribution, with large amount of low disturbance intensity and small share of high-level disturbance intensity. This study explored the effects of multiple sample acquisition methods in building the regression models for cyclone disturbance intensity. Based on the results presented in the study, disproportional stratified sampling method, which ensures adequate representation of samples from the minority strata, is recommended. Similar sampling method can be applied to other type of forest disturbance, including fire, drought, pest and pathogens, and remote sensing image classification (Ramezan et al., 2019).

Our results showed that each cyclone interacted with the landscape in a unique way, so the most significant factor driving the variation in disturbance intensity pattern differs from cyclones. Similar conclusions were found in past cyclone studies with FIA and ground data (Xi et al., 2008a,b). Climate variables are the most dominant factors contributing to the variation in impacts of Katrina and María, and they can explain 15−30% of variance in impacts driven by other two cyclones. Wind and rainfall are both climate factors, but how they interact with the ecosystem is quite different.

Wind interacts with forests and can result in loss of leaves, tree snapping and uprooting (Lugo, 2008). The correlation between wind and forest disturbance severity has also been described in previous studies (Negrón-Juárez et al., 2014a, Foster and Boose, 1992; Lugo, 2008; Xi et al., 2008a,b). Lugo et al. (2000) used kinetic energy to understand the effect of hurricane winds, and they found that the kinetic energy of hurricane winds was 3500 and 15 000 times higher than the energy of average global winds. Wind serves as a strong positive predictor of hurricane damage risk, explaining 58% of variation in tree damage of hurricane Hugo model (Xi et al., 2008a,b). Wind speed were found to be consistent among Katrina, Rita, Gustav, Charley, and María studies, as forest effects increased with maximum wind speed until 120–160 km/h (Negrón-Juárez et al., 2014a, Hall et al., 2019). In this study, we proposed a 40 m/s (144 km/h) wind speed threshold that splits low and high forest disturbance intensity. With maximum wind speed under the threshold, forests experienced low-level disturbance (ΔNPV < 0.2). Once the wind speeds of cyclones passed the threshold, forests were prone to experience strong effects brought by hurricane winds without significant difference. Rainfall interacts with soil, which transport materials away from the stand, result in landslides (Xi et al., 2008a). Rainfall is a strong predictor in damage driven by Rita and María as these two cyclones brought more extreme precipitation. Severe rainfall can result in localized flooding, leading to tree mortality from anoxia (Stanturf et al., 2007). Rain can also accelerate soil erosion and mass movement, which can cause uprooting of large trees, since roots are more dislodged from wet soils (Hall et al., 2020).

The results showed that elevation was the most significant factor driving the spatial variation of Rita and María forests effects, and forests were affected differently by elevation. The impacts from Rita were higher on forests grown at lower elevation. Past studies have similar results that valley bottoms experienced high damage levels due to soil saturation (Xi et al., 2008a,b). Opposite to Rita, forests grown on high elevation, such as slopes and ridge, sustain the greatest level of damage in Puerto Rico. Cyclones are external factors to the forests (Lugo 2008), and the location of landmasses and local topography can affect the power of hurricane wind as well as the impact on forests (Boose et al., 1994, Foster and Boose 1995, Boose et al., 2004, Walker, 1991). Wind speed and direction may be modified by surrounding topographic features, particularly in hilly terrain (Boose et al., 1994). Forests with high wind exposure experience highest disturbance (Negrón-Juárez et al., 2014a, Feng et al., 2020), and landscape patterns of wind exposure depends on the interaction of terrain features and peak wind velocity. Although it is well documented that topography influences hurricane impact at the landscape scale, it is difficult to find an appropriate way to capture the complex interaction between topography and hurricane wind (Xi et al., 2008a,b).

Forests differ in their susceptibilities to damages, and pre-disturbance forests structure and composition determined the range and severity of the hurricane impacts on forests (Xi et al., 2008a,b). PreGV, which represented the forest properties in the preceding year, was a strong predictor in studies of Yasi and María, and explained over 10% variation in studies of Katrina and Rita. Studies on Katrina, Yasi, and María showed that preGV had a consistent positive correlation with hurricane impacts. Xi et al. (2008b) found that hurricane-induced tree mortality was positively correlated with pre-hurricane tree size. However, previous studies showed that damage associated with cyclones varied significantly with tree species (Xi et al., 2008a,b; Chapman et al., 2008), and hurricane disturbance influenced the structure and composition of forests at species-specific level (Cooper-Ellis et al., 1999). Even the same forest species sustained different level of damage from cyclones (Xi et al., 2008a).

6.2. Comparisons between two cyclones at the same location

Although Laura (2020) followed almost the identical path as Rita (2005), forests responded differently to them. In Rita study, forests along Neches, Sabine, and Calcasieu rivers sustained highest level of damage. In Laura study, forests along the cyclone track sustained the most disturbance, and low disturbance intensity and some greening up were found along Neches and Sabine rivers (Fig. 13).

Fig. 13c shows that the highest wind speed of Rita was <35 m/s, which was lower than 90% of Laura's wind speed. While forests near Texas Louisiana border experienced relatively lower wind speed 15 years ago when Rita hit, they received over three times more of rainfall than what Laura brought (Fig. 13d). Therefore, Rita can be characterized by the predominant of rain and Laura was characterized by wind. The alternatives in predominant environmental factor result from the trajectory of cyclone and its development stage when it interacted with the forests. Rain and wind interact but they must be evaluated separately as they have different effects (Lugo, 2008). As we discussed in section 5.1, wind interacts with canopy interface and rain interacts with soil interface, and both interactions are modified by aspect and topography. A detailed feedback system can be found in Lugo, 2008.

Coastal plain forests in Texas suffered the most from Rita (Stanturf et al., 2007). Studies show that an inventory of river bank trees blown into the channel of lower Neches and lower Sabine river (Phillips and Park, 2009). This might because that Rita made landfall just east of Sabine Pass, Texas, which was the inlet connecting the Sabine Lake estuary with Gulf of Mexico. Precipitation from Rita exceeded 184 mm on average and increased runoff and stream-flow in the study area, and the blowdown densities caused by Rita was comparable to the impact of flooding (Phillips and Park, 2009).

6.3. The challenges to build a general cyclone impact model

As shown in the results, our machine learning models didn't give a good prediction of the effects of unseen cyclones on forests. Indeed, we find it exceedingly difficult to build a general cyclone impact model or even a regional cyclone impact model. Similar conclusions were found in past studies using parametric models (Xi et al., 2008a,b; Lugo 2008; Stanturf et al., 2007). First, it is difficult to find a set of general rules that can be applied to all the cyclone disturbances. As we discussed in section 5.1, the significant features that can explain the variance in the disturbance intensity varied by cyclones and locations. The explanatory variables also varied at different scales, stand scale, landscape scale, and regional scale (Xi et al., 2008a). For cyclones made landfall in the same region, it was also unpredictable. For example, the range of Laura wind speed hardly overlapped with the wind speed of training data Rita, so as their precipitation data. How could a model trained on Rita with low wind speed, high precipitation can predict the disturbance intensity of Laura with high wind speed and low precipitation? In addition, Lugo 2008 summarized that a cyclone can interact with vegetation, geologic substrate and topography to trigger further forest disturbance such as tree-fall gaps, landslides, floods depending on the types of forests. Therefore, the evaluation of cyclone involved not only wind and rainfall, but also a variety of other ecosystem disturbances that can dissipate high energy when conditions maximize their effect. It should not be surprising, given the complexity of cyclone coupled with landscapes, soils, and states of affected systems, cyclone effects show so much variation and few consistent generalizations. Climate change could alter the frequency, intensity, and duration of cyclones (Dale et al., 2001) and increase the probability of extreme rainfall rate (Patricola and Wehner 2018). It increases the difficulty for machine learning models to learn and extrapolate on unseen data. Such complexity raised the question whether a general hurricane model exists.

Second, it is hard to get more training data. Field observation data

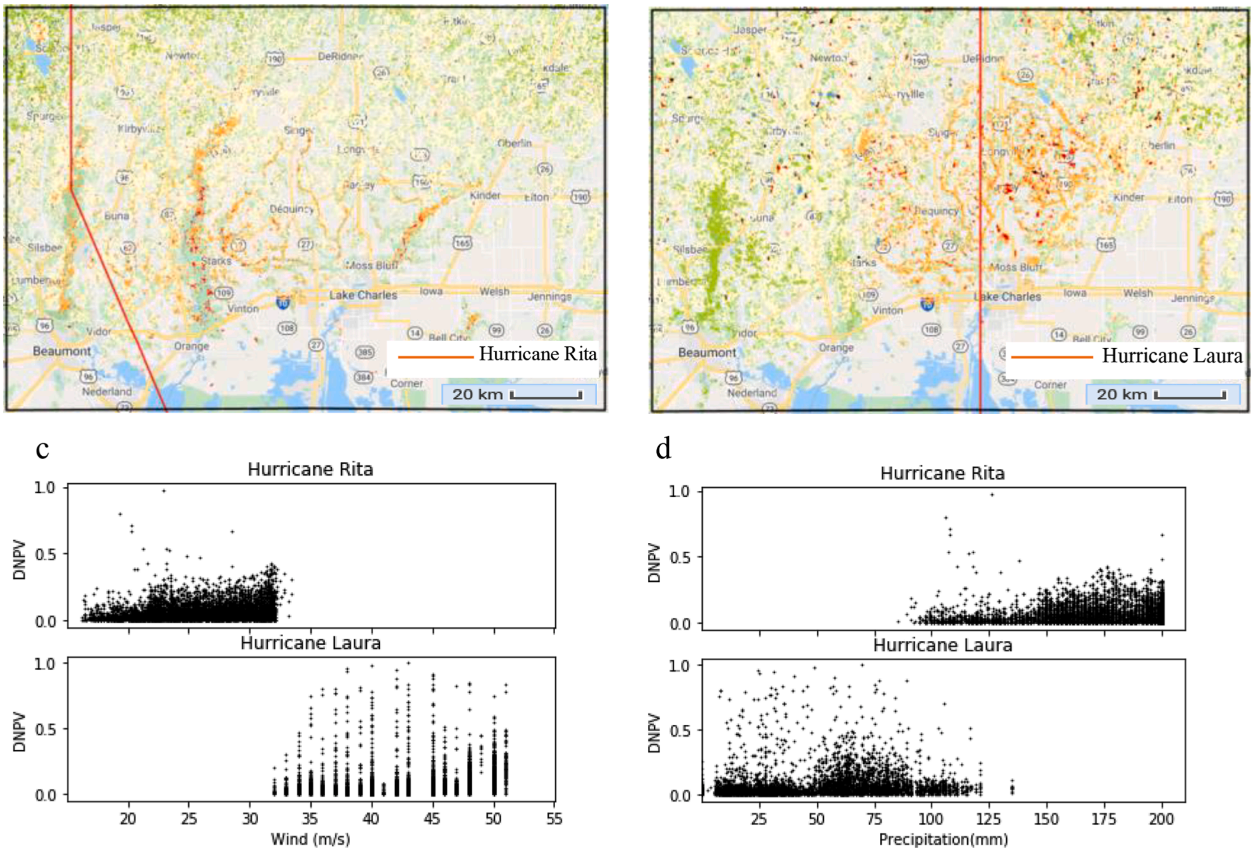

Fig. 13. The comparisons between Rita and Laura. (a) Forest disturbance intensity map of Rita; (b) Forest disturbance intensity map of Laura; (c) The relationship between wind and ΔNPV; (d) The relationship between precipitation and ΔNPV.

are required to validate Landsat-derived ΔNPV metrics, and it is time-consuming to take field samples. Currently we only use 4 hurricanes (Katrina, Rita, Yasi, and María), which have field validated ΔNPV, as our training data. Similar machine learning prediction studies in earth system science have at least 40 examples for training (Mousavi and Beroza, 2020, Corbi et al., 2019). Third, the lack of free access to high resolution wind speed data is another big challenge. H*wind model, developed by Powell et al., 1996, employed a sophisticated compositing technique, which required extensive observation data to produce surface wind data. We only gained access to H*wind data of Katrina, Rita, Yasi (publicly available at Hurricane Research Division before 2013) and María (access under restricted use license of RMS HWIND ENHANCED ARCHIVE), and the data were no longer publicly available after 2013. Without the free access to H*wind data of Michael and Laura, we used HURRECON model to produce wind speed for Michael and Laura. HURRECON model utilized meteorological data to reconstruct wind conditions. For a given location, the model predicts wind speed as a function of storm position, storm speed and direction, eye diameter, maximum wind speed, wind profile constant, and surface type. However, unlike the H*wind, the HURRECON model does not consider local topography and has a much lower resolution. Therefore, HURRECON model is less accurate than H*wind and introduces more uncertainty and errors in the model (Fig. S2). The difference in wind source could be another reason result in the failure of model prediction. Here, we call for more free access to surface wind data such as H*wind.

7. Conclusion

This study used remote sensing data and machine learning models to make comparisons among impacts of 4 cyclones on forests at regional level. It addressed the importance of climate variables, terrain features, and forest properties in predicting tree damage caused by cyclones. Wind, elevation, and pre-disturbance vegetation condition are strong predictors. We found a 40 m/s wind speed threshold that can be generalized on these 4 cyclones, but little consistency can be found on other variables among the studies of different cyclones. Machine learning technologies were used to build cyclone impact models. As machine learning models become more popular in earth science, we showed that them still had limitations in cyclone effects prediction. The models worked well on hold out test data, but they had weak predictability on unseen cyclones. We believed that more finer scale data can be helpful to build local models work with similar ecosystems and landscapes, but the complexities of cyclone effects coupled with landscapes, soils, states of affected systems, climate change lead us to question the existence of an omnipotent cyclone impact model that works for the globe.

Data accessibility statement

The disturbance intensity, wind and preGV maps of Katrina, Rita, Yasi, Maria, Michael, Laura used in this paper can be viewed at https://ylfeng.users.earthengine.app/view/jagfengetal. The scripts supporting the model can be found at https://github.com/ylfeng93/Hurricane-Impact-Model.

CRediT authorship contribution statement

Yanlei Feng: Conceptualization, Methodology, Formal analysis, Investigation, Software, Writing – original draft, Visualization. **Robinson I. Negrón-Juárez:** Conceptualization, Methodology, Data curation, Resources, Investigation, Validation, Writing – review & editing. **Jeffrey Q. Chambers:** Supervision, Conceptualization, Methodology, Writing – review & editing.

Declaration of Competing Interest

The authors declare that they have no known competing financial interests or personal relationships that could have appeared to influence the work reported in this paper.

Acknowledgements

The authors thank the Mark Powell and Risk Management Solutions for creating and maintaining the H*wind Database. The computational work for this study was partially supported by Google cloud free credit. This research was supported as part of the Next Generation Ecosystem Experiments-Tropics (NGEE), funded by the U.S. Department of Energy, Office of Science, Office of Biological and Environmental Research under contract number DE-AC02-05CH11231.

Appendix A. Supplementary material

Supplementary data to this article can be found online at https://doi.org/10.1016/j.jag.2021.102528.

References

Ramezan, C.A., Warner, T.A., Maxwell, A.E., 2019. Evaluation of Sampling and Cross-Validation Tuning Strategies for Regional-Scale Machine Learning Classification. Remote Sens. 11 (2), 185. https://doi.org/10.3390/rs11020185.

Belgiu, M., Drăguţ, L., 2016. Random forest in remote sensing: A review of applications and future directions. ISPRS J. Photogramm. Remote Sens. 114, 24–31.

Birdsey, R.A., Weaver, P.L., 1982. The forest resources of Puerto Rico. USDA Forest Service Resource Bulletin **SO-85**.

Board, O.S. "2 Background of the Gulf Coast System." National Academies of Sciences, Engineering, and Medicine, 2018. Understanding the long-term evolution of the coupled natural-human coastal system: the future of the US Gulf Coast. National Academies Press. doi: 10.17226/25108.

Boose, E.R., Foster, D.R., Fluet, M., 1994. Hurricane impacts to tropical and temperate forest landscapes. Ecol. Monogr. 64 (4), 369–400.

Boose, E.R., Chamberlin, K.E., Foster, D.R., 2001. Landscape and regional impacts of hurricanes in New England. Ecol. Monogr. 71 (1), 27–48.

Boose, E.R., Serrano, M.I., Foster, D.R., 2004. Landscape and regional impacts of hurricanes in Puerto Rico. Ecol. Monogr. 74 (2), 335–352.

Breiman, L., 2001. Statistical modeling: The two cultures (with comments and a rejoinder by the author). Statistical Sci. 16 (3), 199–231.

Brokaw, N.V.L., Walker, L.R., 1991. Summary of the effects of Caribbean hurricanes on vegetation. Biotropica 23 (4), 442. https://doi.org/10.2307/2388264.

Chapman, E.L., Chambers, J.Q., Ribbeck, K.F., Baker, D.B., Tobler, M.A., Zeng, H., White, D.A., 2008. Hurricane Katrina impacts on forest trees of Louisiana's Pearl River basin. For. Ecol. Manage. 256 (5), 883–889.

Chambers, J.Q., Fisher, J.I., Zeng, H., Chapman, E.L., Baker, D.B. and Hurtt, G.C., 2007. Hurricane Katrina's carbon footprint on US Gulf Coast forests. Science, 318(5853), pp.1107-1107.

Cooper-Ellis, S., Foster, D.R., Carlton, G., Lezberg, A., 1999. Forest response to catastrophic wind: results from an experimental hurricane. Ecology 80 (8), 2683–2696.

Corbi, F., Sandri, L., Bedford, J., Funiciello, F., Brizzi, S., Rosenau, M., Lallemand, S., 2019. Machine learning can predict the timing and size of analog earthquakes. Geophys. Res. Lett. 46 (3), 1303–1311.

Dolan, K.A., Hurtt, G.C., Chambers, J.Q., Dubayah, R.O., Frolking, S., Masek, J.G., 2011. Using ICESat's Geoscience Laser Altimeter System (GLAS) to assess large-scale forest disturbance caused by hurricane Katrina. Remote Sens. Environ. 115 (1), 86–96.

Dale, V.H., Joyce, L.A., McNulty, S., Neilson, R.P., Ayres, M.P., Flannigan, M.D., Hanson, P.J., Irland, L.C., Lugo, A.E., Peterson, C.J., Simberloff, D., 2001. Climate change and forest disturbances: climate change can affect forests by altering the frequency, intensity, duration, and timing of fire, drought, introduced species, insect and pathogen outbreaks, hurricanes, windstorms, ice storms, or landslides. Bioscience 51 (9), 723. https://doi.org/10.1641/0006-3568(2001)051[0723:CCAFD]2.0.CO;2.

Feng, Y., Negrón-Juárez, R.I., Chambers, J.Q., 2020. Remote sensing and statistical analysis of the effects of hurricane María on the forests of Puerto Rico. Remote Sens. Environ. 247, 111940. https://doi.org/10.1016/j.rse.2020.111940.

Foster, D.R., Boose, E.R., 1992. Patterns of forest damage resulting from catastrophic wind in central New England, U.S.A. J. Ecol. 80 (1), 79. https://doi.org/10.2307/2261065.

Foster D. R. & Boose E. R., 1995 Hurricane disturbance regimes in temperate and tropical forest ecosystems. In: Wind and Trees (eds M. P. Coutts & J. Grace) pp. 305–38. Cambridge University Press, Cambridge.

Gang, C., Pan, S., Tian, H., Wang, Z., Xu, R., Bian, Z., Pan, N., Yao, Y., Shi, H., 2020. Satellite observations of forest resilience to hurricanes along the northern Gulf of Mexico. For. Ecol. Manage. 472, 118243. https://doi.org/10.1016/j.foreco.2020.118243.

GlobCover products are from ESA 2010 and UCLouvain. http://due.esrin.esa.int/page_globcover.php.

Goldenberg, S.B., Landsea, C.W., Mestas-Nuñez, A.M., Gray, W.M., 2001. The recent increase in Atlantic hurricane activity: Causes and implications. Science 293 (5529), 474–479.

Gislason, P.O., Benediktsson, J.A., Sveinsson, J.R., 2006. Random forests for land cover classification. Pattern Recogn. Lett. 27 (4), 294–300.

Hall, J., Muscarella, R., Quebbeman, A., Arellano, G., Thompson, J., Zimmerman, J.K., Uriarte, M., 2020. Hurricane-induced rainfall is a stronger predictor of tropical forest damage in Puerto Rico than maximum wind speeds. Sci. Rep. 10 (1), 1–10.

Hengl, T., Gupta, S., 2019. Soil water content (volumetric %) for 33kPa and 1500kPa suctions predicted at 6 standard depths (0, 10, 30, 60, 100 and 200 cm) at 250 m resolution (Version v01). Zenodo.

Hengl, T., 2018. Soil texture classes (USDA system) for 6 soil depths (0, 10, 30, 60, 100 and 200 cm) at 250 m (Version v02). Zenodo.

Jarvis, A., H.I. Reuter, A. Nelson, E. Guevara. 2008. Hole-filled SRTM for the globe Version 4, available from the CGIAR-CSI SRTM 90m Database: http://srtm.csi.cgiar.org.

Kim, D., Millington, A.C., Lafon, C.W., 2019. Biotic and spatial factors potentially explain the susceptibility of forests to direct hurricane damage. J. Ecol. Environ. 43 (1), 37.

Kossin, J.P., Emanuel, K.A., Vecchi, G.A., 2014. The poleward migration of the location of tropical cyclone maximum intensity. Nature 509 (7500), 349–352.

Kossin, J.P., 2018. A global slowdown of tropical-cyclone translation speed. Nature 558 (7708), 104–107.

Lugo, A.E., 2008. Visible and invisible effects of hurricanes on forest ecosystems: An international review. Austral Ecol. 33, 368–398.

Lugo, A.E., Rogers, C.S., Nixon, S.W., 2000. Hurricanes, coral reefs and rainforests: resistance, ruin and recovery in the Caribbean. AMBIO J. Human Environ. 29 (2), 106–114.

Mousavi, S.M. and Beroza, G.C., 2020. A machine-learning approach for earthquake magnitude estimation. Geophysical Research Letters, 47(1), p.e2019GL085976.

Negrón-Juárez, R., Baker, D.B., Chambers, J.Q., Hurtt, G.C., Goosem, S., 2014a. Multi-scale sensitivity of Landsat and MODIS to forest disturbance associated with tropical cyclones. Remote Sens. Environ. 140, 679–689.

Negrón-Juárez, R.I., Chambers, J.Q., Guimaraes, G., Zeng, H., Raupp, C.F.M., Marra, D. M., Ribeiro, G.H.P.M., Saatchi, S.S., Nelson, B.W., Higuchi, N., 2010a. Widespread Amazon forest tree mortality from a single cross-basin squall line event. Geophys. Res. Lett. 37 (16) n/a n/a.

Negrón-Juárez, R., Baker, D.B., Zeng, H., Henkel, T.K., Chambers, J.Q., 2010b. Assessing hurricane-induced tree mortality in US Gulf Coast forest ecosystems. J. Geophys. Res. Biogeosci. 115 (G4) https://doi.org/10.1029/2009JG001221.

Negrón-Juárez, R.I., Chambers, J.Q., Hurtt, G.C., Annane, B., Cocke, S., Powell, M., Stott, M., Goosem, S., Metcalfe, D.J., Saatchi, S.S., 2014b. Remote sensing assessment of forest disturbance across complex mountainous terrain: The pattern and severity of impacts of tropical cyclone Yasi on Australian rainforests. Remote Sensing 6 (6), 5633–5649.

Pasch, R. J, Penny, A.B., and Berg, R., 2018. National Hurricane Center Tropical Cyclone Report Hurricane Maria (AL152017). National Hurricane Center. https://www.nhc.noaa.gov/data/tcr/AL152017_Maria.pdf.

Patricola, C.M., Wehner, M.F., 2018. Anthropogenic influences on major tropical cyclone events. Nature 563 (7731), 339–346.

Perry, C.T., Smithers, S.G., Kench, P.S., Pears, B., 2014. Impacts of Cyclone Yasi on nearshore, terrigenous sediment-dominated reefs of the central Great Barrier Reef, Australia. Geomorphology 222, 92–105.

Phillips, J.D., Park, L., 2009. Forest blowdown impacts of Hurricane Rita on fluvial systems. Earth Surf. Process. Landforms 34 (8), 1069–1081.

Powell, M.D., Houston, S.H., Amat, L.R., Morisseau-Leroy, N., 1998. The HRD real-time hurricane wind analysis system. J. Wind Eng. Ind. Aerodyn. 77-78, 53–64.

Powell, M.D., Houston, S.H., Reinhold, T.A., 1996. Hurricane Andrew's landfall in south Florida. Part I: Standardizing measurements for documentation of surface wind fields. Weather Forecasting 11 (3), 304–328.

Russo, S., Lürig, M., Hao, W., Matthews, B., Villez, K., 2020. Active learning for anomaly detection in environmental data. Environ. Modell. Software 134, 104869. https://doi.org/10.1016/j.envsoft.2020.104869.

Simard, M., Pinto, N., Fisher, J., Baccini, A. 2011. Mapping forest canopy height globally with spaceborne lidar. Journal of Geophysical Research. 116: G04021. [doi: 10.1029/2011JG001708] (https://doi.org/10.1029/2011JG001708).

Stanturf, J.A., Goodrick, S.L., Outcalt, K.W., 2007. Disturbance and coastal forests: a strategic approach to forest management in hurricane impact zones. For. Ecol. Manage. 250 (1-2), 119–135.

Thornton, P.E., M.M. Thornton, B.W. Mayer, Y. Wei, R. Devarakonda, R.S. Vose, and R.B. Cook. 2016. Daymet: Daily Surface Weather Data on a 1-km Grid for North America, Version 3. ORNL DAAC, Oak Ridge, Tennessee, USA.

Tan, B., Masek, J.G., Wolfe, R., Gao, F., Huang, C., Vermote, E.F., Sexton, J.O., Ederer, G., 2013. Improved forest change detection with terrain illumination corrected Landsat images. Remote Sens. Environ. 136, 469–483.

Theobald, D.M., Harrison-Atlas, D., Monahan, W.B., Albano, C.M., Carmel, Y., 2015. Ecologically-relevant maps of landforms and physiographic diversity for climate adaptation planning. PLoS ONE 10 (12), e0143619.

Uriarte, M., Thompson, J., Zimmerman, J.K., 2019. Hurricane María tripled stem breaks and doubled tree mortality relative to other major storms. Nat. Commun. 10 (1), 1–7.
Xi, W., Peet, R.K., Decoster, J.K., Urban, D.L., 2008a. Tree damage risk factors associated with large, infrequent wind disturbances of Carolina forests. Forestry 81 (3), 317–334.
Xi, W., Peet, R.K., Urban, D.L., 2008b. Changes in forest structure, species diversity and spatial pattern following hurricane disturbance in a Piedmont North Carolina forest, USA. J. Plant Ecol. 1 (1), 43–57.